2007 IEEE International Conference on
Robotics and Automation
Roma, Italy, 10-14 April 2007

Dynamic Modelling for Planar Extensible Continuum Robot Manipulators

Enver Tatlicioglu, Ian D. Walker†, and Darren M. Dawson

Abstract: In this paper, a new dynamic model for continuum robot manipulators is derived. The dynamic model is developed based on the geometric model of extensible continuum robot manipulators with no torsional effects. The development presented in this paper is an extension of the dynamic model proposed in [20] (by Mochiyama and Suzuki) to include a class of extensible continuum robot manipulators. Numerical simulation results are presented for a planar 3-link extensible continuum robot manipulator.

I. Introduction

In most engineered systems, the behaviour of the system is required to be accurately modelled to improve the performance of the system. In many applications, design simulation and proposed control algorithms require more than just a simple kinematic or dynamic model [2]. Not only an accurate model but a real-time calculation of the dynamic model is also needed for control algorithms or simulations.

The desire to enhance the performance of robot manipulators resulted in a renewed interest in continuum robots [23]. To our best knowledge, the concept of continuum robot was first introduced in the 1960's [1]. Numerous designs of continuum robots were presented in [4], [6], [9], [12], and [16]. Recently, there has been an increasing interest in designing 'biologically inspired' continuum robots. Some of these designs are mimicking trunks [8], [27], tentacles [18], [22], [25] and snakes [9]. Several commercial implementations have appeared (i.e., [3] and [10]).

The results in this paper are motivated by and are applicable to the OCTARM continuum manipulator. The OCTARM manipulator is a biologically inspired soft robot manipulator resembling an elephant trunk or an octopus arm [19]. The OCTARM, shown in Figure 1, is a three-section robot with nine degrees of freedom. Aside from two axis bending with constant curvature, each section is also capable of extension. The bending and extension capabilities of OCTARM makes it suitable for a wide variety of physical applications ranging from whole arm grasping of various shapes of payloads to navigation of unstructured environments [18] and provides an increased workspace compared to its inextensible counterparts [28]. In [13], Jones and Walker presented a kinematic model for a general class of continuum robots. While the kinematic model proposed in [13] is applicable to OCTARM, none of the dynamic models proposed in current literature meets the demands. The modelling of dynamic behaviour of extensible (variable length) continuum robot manipulators is an important open research area.

There has been previous research in dynamic modelling of biologically inspired robot manipulators. In two recent papers [15], [17], the authors presented dynamic models for snake-like robots. However, in both cases, hyper-redundant serial rigid-link systems are considered. This does not model the continuous nature of continuum robots. In [29], researchers presented a 2-D dynamic model for the octopus arm. However, while allowing extensibility, the model is based on an approximation (by a finite number of linear models) to the true continuum case. In [6], Chirikjian and Burdick considered extensibility of hyper-redundant manipulators. A kinematic model was presented based on the modal approach introduced in [7] and a dynamic model was proposed in [5]. In [11], Ivanescu et. al proposed a dynamic model for an extensible tentacle arm. However, the dynamic model proposed in [5] for 3-D case remains in integral differential form, which makes it problematic for real-time control and the dynamic model in [11] was derived based on the restrictive assumption that the manipulator does not bend past a small-strain region. In [20] and [21], Mochiyama and Suzuki presented a three-dimensional dynamic model for an inextensible (constant length) continuum manipulator, considering the continuum robot as a combination of slices where each slice is a rigid link. To derive the dynamic model, limit of a serial rigid chain model is obtained as the kinematic degrees of freedom goes to infinity. However, the dynamic model does not include extensible manipulators.

In this paper, the work in [20] is modified and extended in order to include the important class of extensible continuum robot manipulators. A geometric model of a 3-link extensible continuum robot manipulator with a circular cross-section is considered (see Figure 2). For simplicity, the geometric model is assumed to have no torsional effects. After presenting the system model and model properties, the kinetic energy of a slice of the continuum robot is evaluated. The total kinetic energy of the manipulator is obtained by utilizing a limit operation (i.e., sum of the kinetic energy of the slices). By utilizing a Lagrange representation, the dynamic model of a planar 3-link extensible continuum robot manipulator is obtained. It is also proved that the skew-symmetry property is satisfied for the presented dynamic model (i.e., $(\dot{M}(q) - 2V(q,\dot{q}))$ is skew-symmetric). Numerical simulation results are presented for a planar 3-link extensible continuum robot manipulator.

This work is supported in part by a DOC Grant, an ARO Automotive Center Grant, a DOE Contract, a Honda Corporation Grant, and by the Defense Advanced Research Projects Agency (DARPA), Contract Number N66001-C-8043.

The authors are with the Department of Electrical & Computer Engineering, Clemson University, Clemson, SC 29634-0915.
E-mail: [etatlic,ianw,ddawson]@ces.clemson.edu
†Corresponding Author: Phone: 864-656-7209; Fax: 864-656-7220

II. System Model and Properties

The geometric model of a 3-link extensible continuum robot manipulator utilized in this paper is presented in Figure 2. This geometric model is a good model of OCTARM, a soft continuum robot manipulator, which is shown in Figure 1.

The following convention, which is adopted from [20], will be adhered throughout the following development[1]. The matrix, ${}^{0}\Phi(0) \in SO(3)$ represents the orientation matrix of the base frame, and ${}^{0}p(0) \in \mathbb{R}^3$ represents the position vector of the origin. The matrices, ${}^{0}\Phi(\sigma,t), {}^{\xi}\Phi(\sigma,t) \in SO(3)$ represent the orientation matrices of the extended Frenet frame at σ relative to the base frame and ${}^{\xi}\Phi(\xi,t) \in SO(3)$, respectively. The vectors, ${}^{0}p(\sigma,t), {}^{\xi}p(\sigma,t) \in \mathbb{R}^3$ represent the position vectors of the point σ relative to the origin as viewed from the base frame and ${}^{\xi}\Phi(\xi,t)$, respectively. For simplicity, the notation of $\Phi(\sigma,t)$ and $p(\sigma,t)$ will be preferred instead of ${}^{\sigma}\Phi(\sigma,t)$ and ${}^{\sigma}p(\sigma,t)$ throughout the rest of the paper. The section lengths of the manipulator are denoted as $d_i(t) \in \mathbb{R}_+$, $i = 1,2,3$, and $\kappa(\sigma,t) \in \mathbb{R}$ represents the curvature of the point σ. The total length of the robot manipulator, denoted as $d(t) \in \mathbb{R}_+$, is equal to the following

$$d(t) \triangleq d_1(t) + d_2(t) + d_3(t). \tag{1}$$

The system model is assumed to satisfy the following properties.

Property 1: The curvature κ of each point σ of the manipulator is a function of both time and σ. Consistent with the OCTARM, it is assumed that the curvature of a link is only function of time (i.e., $\kappa(\sigma,t) = \kappa_i(t)$ if σ is a point on Link i, $i = 1,2,3$). It is assumed in the analysis that the curvature is always non-zero[2] (i.e., $\kappa(\sigma,t) \neq 0 \; \forall (\sigma,t)$).

Property 2: In Figure 2, $p(\xi,t) \in \mathbb{R}^3$ is the position vector of point ξ of the backbone curve and $p_c(\xi,t) \in \mathbb{R}^3$ is the position vector of the center of mass of the slice at ξ. Again consistent with the OCTARM, it is assumed that $p(\xi,t)$ and $p_c(\xi,t)$ coincide (i.e., $\Delta p(\xi) = \begin{bmatrix} 0 & 0 & 0 \end{bmatrix}^T$).

Property 3: The mass density of the robot manipulator is uniform. The line mass density of the slice, denoted as $m(\sigma,t) \in \mathbb{R}$, is defined as follows

$$m(\sigma,t) = \frac{m}{d(t)} \tag{2}$$

where $m \in \mathbb{R}$ is the total mass of the manipulator.

Property 4: Since the system is assumed to be planar with no torsional effects, then the system has no gravitational potential energy.

[1]To set a basis for our future work three-dimensional space is preferred for representing the orientation and velocity instead of their two-dimensional counterparts.

[2]It should be noted that straight out (i.e., when the links are straight) is a kinematic singularity as well. The reader is referred to [14] for a detailed analysis to overcome this singularity.

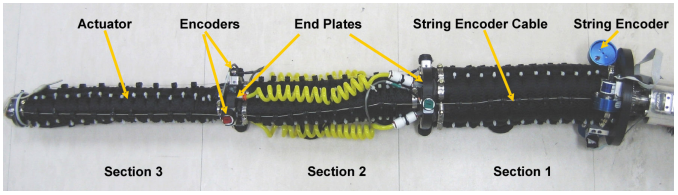

Fig. 1. Octarm Continuum Robot (ver. 5.2) in Clemson University Mechatronics Laboratory

III. Dynamic Modelling

The orientation matrix of the extended Frenet frame at σ with respect to the base frame, denoted as ${}^{0}\Phi(\sigma,t)$, is given as follows

$${}^{0}\Phi(\sigma,t) = \begin{bmatrix} \cos(\sigma\kappa(\sigma,t)) & 0 & -\sin(\sigma\kappa(\sigma,t)) \\ 0 & 1 & 0 \\ \sin(\sigma\kappa(\sigma,t)) & 0 & \cos(\sigma\kappa(\sigma,t)) \end{bmatrix} \tag{3}$$

The orientation matrix given in (3) is equal to the orientation matrix provided in Equation (8) of [13] with the angle of curvature is equal to zero (i.e., $\phi(\sigma,t) = 0$). The change of the orientation matrix along the manipulator is characterized by the following equation

$$\frac{\partial\, {}^{0}\Phi(\sigma,t)}{\partial\sigma} = {}^{0}\Phi(\sigma,t)\, a^{\times}(\sigma,t) \tag{4}$$

where $a^{\times}(\sigma,t) \in \mathbb{R}^{3\times3}$ is the skew-symmetric matrix of the frame rate vector $a(\sigma,t) \in \mathbb{R}^3$. After utilizing (3) and (4), $a(\sigma,t)$ and $a^{\times}(\sigma,t)$ can be defined as follows

$$\begin{aligned} a(\sigma,t) &= \begin{bmatrix} 0 \\ -\kappa(\sigma,t) \\ 0 \end{bmatrix}, \\ a^{\times}(\sigma,t) &= \begin{bmatrix} 0 & 0 & -\kappa(\sigma,t) \\ 0 & 0 & 0 \\ \kappa(\sigma,t) & 0 & 0 \end{bmatrix}. \end{aligned} \tag{5}$$

The position vector of the point σ from the origin $p(0)$ with respect to the base frame, denoted as ${}^{0}p(\sigma,t)$, is evaluated as follows

$${}^{0}p(\sigma,t) = \int_0^{\sigma} {}^{0}\Phi(\eta,t)\, e_{\times}\, d\eta \tag{6}$$

where $e_{\times} \triangleq \begin{bmatrix} 1 & 0 & 0 \end{bmatrix}^T$. The orientation matrix of the extended Frenet frame at σ relative to $\Phi(\xi,t)$, denoted as ${}^{\xi}\Phi(\sigma,t)$, is calculated as follows

$${}^{\xi}\Phi(\sigma,t) \triangleq {}^{0}\Phi^{T}(\xi,t)\; {}^{0}\Phi(\sigma,t). \tag{7}$$

The position vector of the point σ relative to the origin as viewed from $\Phi(\xi,t)$, denoted as ${}^{\xi}p(\sigma,t)$, is evaluated as follows

$${}^{\xi}p(\sigma,t) \triangleq {}^{0}\Phi^{T}(\xi,t)\; {}^{0}p(\sigma,t). \tag{8}$$

The internal variable vector at σ which is denoted as $\theta(\sigma,t) \in \mathbb{R}^2$ is defined as follows

$$\theta(\sigma,t) \triangleq \begin{bmatrix} l(\sigma,t) \\ \kappa(\sigma,t) \end{bmatrix} \tag{9}$$

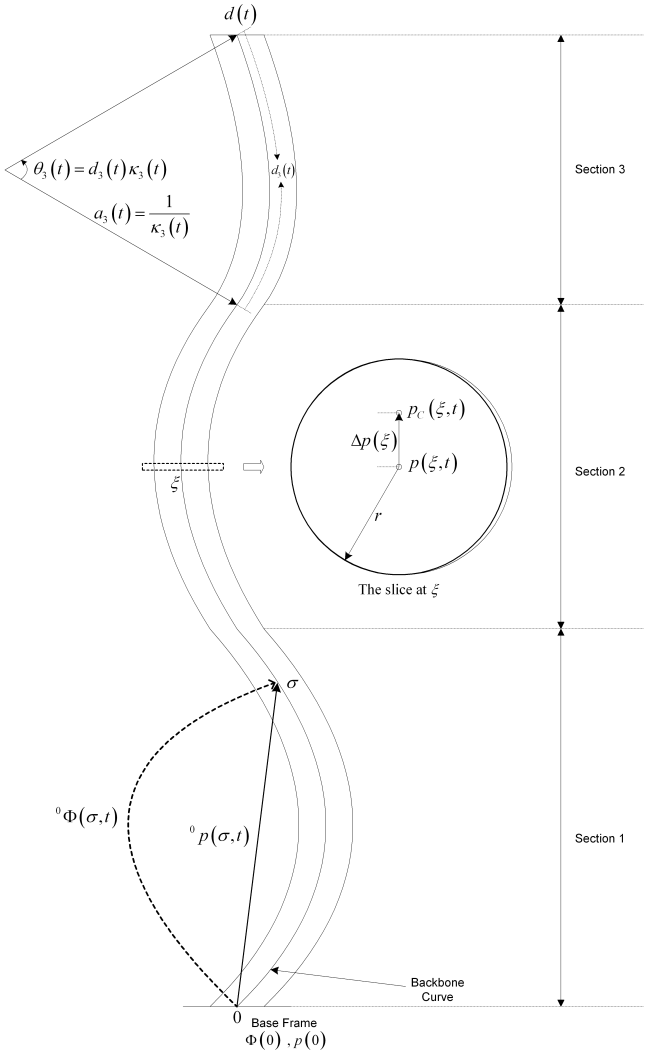

Fig. 2. Geometry of a 3-Link Extensible Robot Manipulator

where $l(\sigma,t)$ and $\kappa(\sigma,t)$ reflect the extension and curvature of the model. The extended axis matrix $\overline{A}(\theta(\sigma,t)) \in \mathbb{R}^{6\times 2}$ is defined as follows

$$\overline{A}(\theta(\sigma,t)) \triangleq \begin{bmatrix} 1 & 0 & 0 & 0 & 0 & 0 \\ 0 & 0 & 0 & 0 & -1 & 0 \end{bmatrix}^T. \quad (10)$$

So far, the main extension of this development over [20] is the definition of the internal variable vector. The extensibility of our model is reflected by designing $\theta(\sigma,t)$ to include $l(\sigma,t)$. This design allows the model to extend in each section, which results in a variable total length, while the geometric model presented in [20] had a constant total length. As a consequence of this new design for the internal variable vector, the extended axis matrix is modified accordingly. The adjoint matrix $Ad_{g(\sigma,\eta,t)} \in \mathbb{R}^{6\times 6}$ in terms of the rigid body transformation $g(\sigma,\eta,t) \in SE(3)$ is defined as follows

$$Ad_{g(\sigma,\eta,t)} \triangleq \begin{bmatrix} {}^{\sigma}\Phi(\eta,t) & \\ 0_{3\times 3} & \\ ({}^{\sigma}p^{\times}(\eta,t) - {}^{\sigma}p^{\times}(\sigma,t))\ {}^{\sigma}\Phi(\eta,t) & \\ {}^{\sigma}\Phi(\eta,t) & \end{bmatrix} \quad (11)$$

where $0_{3\times 3} \in \mathbb{R}^{3\times 3}$ is a matrix of zeros. The kinetic energy of the slice at σ (see Figure 2) is given as follows [20]

$$K(\sigma,t) \triangleq \frac{1}{2}\int_0^{\sigma}\int_0^{\sigma} \frac{\partial\theta^T(\eta,t)}{\partial t}\overline{A}^T(\eta,t)\, Ad^T_{g(\sigma,\eta,t)} \quad (12)$$
$$M(\sigma,t)\, Ad_{g(\sigma,\xi,t)}\overline{A}(\xi,t)\frac{\partial\theta(\xi,t)}{\partial t} d\eta d\xi$$

where $M(\sigma,t) \in \mathbb{R}^{6\times 6}$ is the inertia matrix of the slice at σ which is defined as follows

$$M(\sigma,t) \triangleq \begin{bmatrix} m(\sigma,t) I_3 & -m(\sigma,t)\Delta p^{\times}(\sigma) \\ m(\sigma,t)\Delta p^{\times}(\sigma) & I(\sigma) \end{bmatrix} \quad (13)$$

where $m(\sigma,t)\Delta p(\sigma) \in \mathbb{R}^3$ is the first moment of inertia of the slice, $I(\sigma) \in \mathbb{R}^{3\times 3}$ is the inertia tensor of the slice, and $I_3 \in \mathbb{R}^{3\times 3}$ is the standard identity matrix. The inertia tensor of the slice is assumed to be of the following form

$$I(\sigma) \triangleq \frac{mr^2}{2d}\begin{bmatrix} 1 & 0 & 0 \\ 0 & 0 & 0 \\ 0 & 0 & 0 \end{bmatrix} \quad (14)$$

where r is the radius of the circular cross-section of the robot manipulator. After utilizing Properties 1 and 2, the inertia matrix of the slice at σ can be evaluated as follows

$$M(\sigma,t) = diag\left\{\frac{m}{d}, \frac{m}{d}, \frac{m}{d}, \frac{mr^2}{2d}, 0, 0\right\}. \quad (15)$$

Due to the piecewise definition of the curvature (see Property 1), the kinetic energy of the slice at σ which is formulated by (12) will not be evaluated explicitly. However, by sliding the slice at σ over every section of the manipulator, the kinetic energy of every slice at σ can be calculated. The expression in (12) can be rewritten as follows

$$K(\sigma,t) = \int_0^{\sigma}\int_0^{\sigma} I(\sigma,\eta,\xi,t)\, d\eta d\xi \quad (16)$$

where $I(\sigma,\eta,\xi,t)$ is the integrand defined as follows

$$\begin{aligned} I \triangleq \frac{m}{2d}\Big\{ & \dot{l}(\xi,t)\,\dot{l}(\eta,t)\cos(\xi\kappa(\xi,t) - \eta\kappa(\eta,t)) \quad (17)\\ & + \dot{l}(\xi,t)\,\dot{\kappa}(\eta,t)\left[\left(\frac{1}{\kappa(\eta,t)} - \frac{1}{\kappa(\sigma,t)}\right)\cos(\xi\kappa(\xi,t))\right.\\ & + \frac{1}{\kappa(\sigma,t)}\cos(\xi\kappa(\xi,t) - \sigma\kappa(\sigma,t))\\ & \left. - \frac{1}{\kappa(\eta,t)}\cos(\xi\kappa(\xi,t) - \eta\kappa(\eta,t))\right]\\ & + \dot{\kappa}(\xi,t)\,\dot{l}(\eta,t)\left[\left(\frac{1}{\kappa(\xi,t)} - \frac{1}{\kappa(\sigma,t)}\right)\cos(\eta\kappa(\eta,t))\right.\\ & + \frac{1}{\kappa(\sigma,t)}\cos(\sigma\kappa(\sigma,t) - \eta\kappa(\eta,t))\\ & \left. - \frac{1}{\kappa(\xi,t)}\cos(\xi\kappa(\xi,t) - \eta\kappa(\eta,t))\right] \end{aligned}$$

$$
\begin{aligned}
&+\dot{\kappa}(\xi,t)\,\dot{\kappa}(\eta,t)\\
&\left[\frac{1}{\kappa(\sigma,t)}\left(\frac{1}{\kappa(\xi,t)}+\frac{1}{\kappa(\eta,t)}-\frac{2}{\kappa(\sigma,t)}\right)\cos(\sigma\kappa(\sigma,t))\right.\\
&+\frac{1}{\kappa(\xi,t)}\left(\frac{1}{\kappa(\sigma,t)}-\frac{1}{\kappa(\eta,t)}\right)\cos(\xi\kappa(\xi,t))\\
&-\frac{1}{\kappa(\xi,t)}\frac{1}{\kappa(\sigma,t)}(1+\cos(\xi\kappa(\xi,t)-\sigma\kappa(\sigma,t)))\\
&-\frac{1}{\kappa(\eta,t)}\frac{1}{\kappa(\sigma,t)}(1+\cos(\sigma\kappa(\sigma,t)-\eta\kappa(\eta,t)))\\
&+\frac{1}{\kappa(\eta,t)}\left(\frac{1}{\kappa(\sigma,t)}-\frac{1}{\kappa(\xi,t)}\right)\cos(\eta\kappa(\eta,t))\\
&\left.+\frac{2}{\kappa^2(\sigma,t)}\right]\Bigg\}.
\end{aligned}
$$

The total kinetic energy of the system is defined as follows

$$K(t)\triangleq\int_0^{d(t)}K(\sigma,t)\,d\sigma \tag{18}$$

where $K(\sigma,t)$ is the kinetic energy of the slice at σ. The upper limit of the integral in (18) is the total length of the manipulator, which is a function of time as a result of the extensible nature of our geometric model. However, the total length of the manipulator in [20] was constant. To facilitate the subsequent development, the total kinetic energy of the system will be rewritten as follows

$$
\begin{aligned}
K(t) &= \int_0^{d_1(t)}K_1(\sigma,t)\,d\sigma+\int_{d_1(t)}^{d_2(t)}K_2(\sigma,t)\,d\sigma\\
&\quad+\int_{d_2(t)}^{d_3(t)}K_3(\sigma,t)\,d\sigma
\end{aligned}\tag{19}
$$

where $K_i(\sigma,t)$ is the kinetic energy of slice σ when σ is a point on Link i, $i=1,2,3$. To facilitate the subsequent development $I_{ijk}(\sigma,\eta,\xi,t)$ is defined as follows

$$I_{ijk}(\sigma,\eta,\xi,t)\triangleq I(\sigma,\eta,\xi,t)|_{\sigma\in\text{ Link }i,\eta\in\text{ Link }j,\xi\in\text{ Link }k} \tag{20}$$

where for any $s\in$ Link i means $\dot{l}(s)=\dot{d}_i(t)$ and $\kappa(s)=\kappa_i(t)$. After utilizing (16), (19), (20) along with Property 1, $K_i(\sigma,t)$, $i=1,2,3$ can be evaluated as follows[3]

$$K_1=\int_0^{\sigma}\int_0^{\sigma}I_{111}\,d\eta\,d\xi \tag{21}$$

$$
\begin{aligned}
K_2=&\int_0^{d_1(t)}\int_0^{d_1(t)}I_{211}\,d\eta\,d\xi+\int_0^{d_1(t)}\int_{d_1(t)}^{\sigma}I_{221}\,d\eta\,d\xi\\
&+\int_{d_1(t)}^{\sigma}\int_0^{d_1(t)}I_{212}\,d\eta\,d\xi+\int_{d_1(t)}^{\sigma}\int_{d_1(t)}^{\sigma}I_{222}\,d\eta\,d\xi
\end{aligned}\tag{22}
$$

[3]For simplicity, I_{ijk} is preferred instead of $I_{ijk}(\sigma,\eta,\xi,t)$, in (21), (22), and (23).

$$
\begin{aligned}
K_3=&\int_0^{d_1(t)}\int_0^{d_1(t)}I_{311}\,d\eta\,d\xi+\int_0^{d_1(t)}\int_{d_1(t)}^{d_2(t)}I_{321}\,d\eta\,d\xi\\
&+\int_0^{d_1(t)}\int_{d_2(t)}^{\sigma}I_{331}\,d\eta\,d\xi+\int_{d_1(t)}^{d_2(t)}\int_0^{d_1(t)}I_{312}\,d\eta\,d\xi\\
&+\int_{d_1(t)}^{d_2(t)}\int_{d_1(t)}^{d_2(t)}I_{322}\,d\eta\,d\xi+\int_{d_1(t)}^{d_2(t)}\int_{d_2(t)}^{\sigma}I_{332}\,d\eta\,d\xi\\
&+\int_{d_2(t)}^{\sigma}\int_0^{d_1(t)}I_{313}\,d\eta\,d\xi+\int_{d_2(t)}^{\sigma}\int_{d_1(t)}^{d_2(t)}I_{323}\,d\eta\,d\xi\\
&+\int_{d_2(t)}^{\sigma}\int_{d_2(t)}^{\sigma}I_{333}\,d\eta\,d\xi.
\end{aligned}\tag{23}
$$

To facilitate the subsequent development the joint position vector $q(t)\in\mathbb{R}^6$ is defined as follows

$$q\triangleq\begin{bmatrix}d_1 & d_2 & d_3 & \kappa_1 & \kappa_2 & \kappa_3\end{bmatrix}^T. \tag{24}$$

After utilizing (17), (19)-(23), the total energy of the system can be evaluated as follows

$$
\begin{aligned}
K(t) &= K_{\dot{d}_1\dot{d}_1}\left(\dot{d}_1\right)^2+K_{\dot{d}_1\dot{d}_2}\dot{d}_1\dot{d}_2+K_{\dot{d}_1\dot{d}_3}\dot{d}_1\dot{d}_3\\
&\quad+K_{\dot{d}_1\dot{\kappa}_1}\dot{d}_1\dot{\kappa}_1+K_{\dot{d}_1\dot{\kappa}_2}\dot{d}_1\dot{\kappa}_2+K_{\dot{d}_1\dot{\kappa}_3}\dot{d}_1\dot{\kappa}_3\\
&\quad+K_{\dot{d}_2\dot{d}_2}\left(\dot{d}_2\right)^2+K_{\dot{d}_2\dot{d}_3}\dot{d}_2\dot{d}_3+K_{\dot{d}_2\dot{\kappa}_1}\dot{d}_2\dot{\kappa}_1\\
&\quad+K_{\dot{d}_2\dot{\kappa}_2}\dot{d}_2\dot{\kappa}_2+K_{\dot{d}_2\dot{\kappa}_3}\dot{d}_2\dot{\kappa}_3+K_{\dot{d}_3\dot{d}_3}\left(\dot{d}_3\right)^2\\
&\quad+K_{\dot{d}_3\dot{\kappa}_1}\dot{d}_3\dot{\kappa}_1+K_{\dot{d}_3\dot{\kappa}_2}\dot{d}_3\dot{\kappa}_2+K_{\dot{d}_3\dot{\kappa}_3}\dot{d}_3\dot{\kappa}_3\\
&\quad+K_{\dot{\kappa}_1\dot{\kappa}_1}(\dot{\kappa}_1)^2+K_{\dot{\kappa}_1\dot{\kappa}_2}\dot{\kappa}_1\dot{\kappa}_2+K_{\dot{\kappa}_1\dot{\kappa}_3}\dot{\kappa}_1\dot{\kappa}_3\\
&\quad+K_{\dot{\kappa}_2\dot{\kappa}_2}(\dot{\kappa}_2)^2+K_{\dot{\kappa}_2\dot{\kappa}_3}\dot{\kappa}_2\dot{\kappa}_3+K_{\dot{\kappa}_3\dot{\kappa}_3}(\dot{\kappa}_3)^2.
\end{aligned}\tag{25}
$$

In (25), the terms $K_{\dot{q}_i\dot{q}_j}$ with q_i and q_j being entries of $q(t)$, are presented in [26].

IV. Lagrangian Representation

The Lagrangian of the system is defined as follows

$$L(t)\triangleq K(t) \tag{26}$$

where Property 4 was utilized. Euler-Lagrange equations of motion are defined as follows [24]

$$\frac{d}{dt}\frac{\partial L}{\partial\dot{q}_i}-\frac{\partial L}{\partial q_i}=\tau_i\ ,\ i=1,2,...,6. \tag{27}$$

After utilizing (27), the dynamic model of the system is developed as follows

$$M(q)\,\ddot{q}+V(q,\dot{q})\,\dot{q}=\tau(t) \tag{28}$$

where $M(q)$, $V(q,\dot{q})\in\mathbb{R}^{6\times6}$ are the inertia matrix and centripetal-coriolis terms, respectively, and $\tau(t)\in\mathbb{R}^6$ is the control input. The inertia matrix $M(q)$ and the centripetal-coriolis terms $V(q,\dot{q})$ are defined as follows

$$M(q) \triangleq \tag{29}$$

$$\begin{bmatrix} 2K_{\dot{d}_1\dot{d}_1} & K_{\dot{d}_1\dot{d}_2} & K_{\dot{d}_1\dot{d}_3} & K_{\dot{d}_1\dot{\kappa}_1} & K_{\dot{d}_1\dot{\kappa}_2} & K_{\dot{d}_1\dot{\kappa}_3} \\ K_{\dot{d}_1\dot{d}_2} & 2K_{\dot{d}_2\dot{d}_2} & K_{\dot{d}_2\dot{d}_3} & K_{\dot{d}_2\dot{\kappa}_1} & K_{\dot{d}_2\dot{\kappa}_2} & K_{\dot{d}_2\dot{\kappa}_3} \\ K_{\dot{d}_1\dot{d}_3} & K_{\dot{d}_2\dot{d}_3} & 2K_{\dot{d}_3\dot{d}_3} & K_{\dot{d}_3\dot{\kappa}_1} & K_{\dot{d}_3\dot{\kappa}_2} & K_{\dot{d}_3\dot{\kappa}_3} \\ K_{\dot{d}_1\dot{\kappa}_1} & K_{\dot{d}_2\dot{\kappa}_1} & K_{\dot{d}_3\dot{\kappa}_1} & 2K_{\dot{\kappa}_1\dot{\kappa}_1} & K_{\dot{\kappa}_1\dot{\kappa}_2} & K_{\dot{\kappa}_1\dot{\kappa}_3} \\ K_{\dot{d}_1\dot{\kappa}_2} & K_{\dot{d}_2\dot{\kappa}_2} & K_{\dot{d}_3\dot{\kappa}_2} & K_{\dot{\kappa}_1\dot{\kappa}_2} & 2K_{\dot{\kappa}_2\dot{\kappa}_2} & K_{\dot{\kappa}_2\dot{\kappa}_3} \\ K_{\dot{d}_1\dot{\kappa}_3} & K_{\dot{d}_2\dot{\kappa}_3} & K_{\dot{d}_3\dot{\kappa}_3} & K_{\dot{\kappa}_1\dot{\kappa}_3} & K_{\dot{\kappa}_2\dot{\kappa}_3} & 2K_{\dot{\kappa}_3\dot{\kappa}_3} \end{bmatrix}$$

$$V(q,\dot{q}) \triangleq \begin{bmatrix} V_{11} & V_{12} & V_{13} & V_{14} & V_{15} & V_{16} \\ V_{21} & V_{22} & V_{23} & V_{24} & V_{25} & V_{26} \\ V_{31} & V_{32} & V_{33} & V_{34} & V_{35} & V_{36} \\ V_{41} & V_{42} & V_{43} & V_{44} & V_{45} & V_{46} \\ V_{51} & V_{52} & V_{53} & V_{54} & V_{55} & V_{56} \\ V_{61} & V_{62} & V_{63} & V_{64} & V_{65} & V_{66} \end{bmatrix} \tag{30}$$

where the entries of the inertia matrix and centripetal-coriolis terms are presented in [26].

Remark 1: The inertia matrix $M(q)$ and the centripetal coriolis terms $V(q,\dot{q})$ satisfy the following property:

$$\xi^T \left(\dot{M} - 2V\right)\xi = 0,\ \forall \xi \in \mathbb{R}^6. \tag{31}$$

When, the matrix $(\dot{M} - 2V)$ is skew-symmetric, then (31) is satisfied. The proof of $(\dot{M} - 2V)$ being skew-symmetric is provided in [26].

V. Numerical Results

To underline the validity of the proposed dynamic model, two numerical simulations are presented[4]. In both simulations, the model presented in (28)-(30) is utilized. The model is implemented in Matlab 7.0. In the first simulation, to illustrate the extensibility in the model, the system is fed with $\tau_3(t)$ being a step function with an amplitude of 10^{-4} $[Nm]$ for a duration of 5 seconds, while the other entries of $\tau(t)$ are set to zero. While the changes in the curvatures are negligible, the section lengths are presented in Figure 3. From Figure 3, it is clear that the third section extends appropriately as expected. In the second simulation, to illustrate both bending and extending capabilities as well as the dynamic behaviour of the model, the system is fed with the control input presented in Figures 4 and 5. From Figure 6, it can easily be seen that the third section is extended, and from Figure 7, it is clear how the third section is bent (i.e., the radius of curvature is approximately 0.85 $[m]$ at the end of the simulation run). The changes in d_2, κ_1 and κ_2 illustrate the results of the dynamic input and coupling between the sections. However, it should be noted that the movements observed in κ_1 and κ_2 are negligible (i.e., the radii of curvature are approximately 10 $[m]$ for both cases). Aside from the presented results, also the dynamic model is observed for commonly used properties in the performed simulations. In both cases, the dynamic model satisfied the skew-symmetry property, and the inertia matrix always has a positive determinant as expected.

[4]It should be noted that for the initial conditions utilized in this section the robot manipulator never goes to a straight out singular configuration.

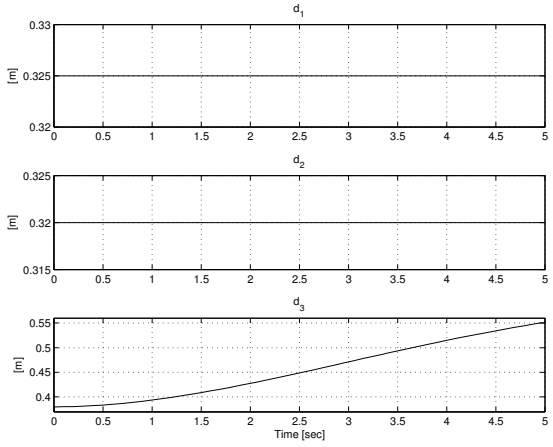

Fig. 3. The section lengths for the first simulation

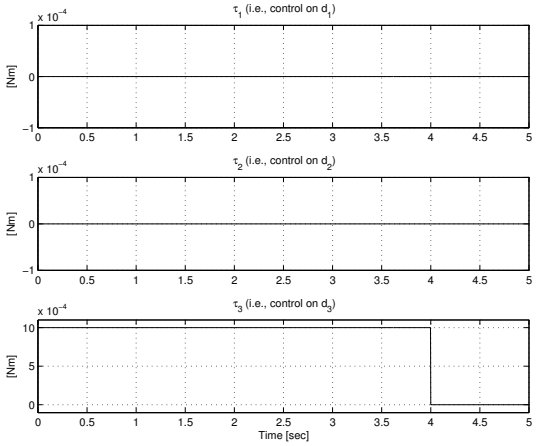

Fig. 4. The control inputs for section lengths (i.e., $\tau_1(t)$, $\tau_2(t)$, $\tau_3(t)$)

VI. Conclusions

A novel dynamic model for planar extensible continuum robot manipulators was derived. First, the kinetic energy of a slice of the continuum robot was evaluated. Then, the total kinetic energy of the manipulator was obtained by utilizing a limit operation (i.e., sum of the kinetic energy of all the slices). Finally, the dynamic model of a planar 3-link extensible continuum robot manipulator was derived, by utilizing the Lagrange representation. Numerical simulation results were presented.

References

[1] V. C. Anderson and R. C. Horn, "Tensor Arm Manipulator Design", *Transactions of the ASME*, vol. 67-DE-57, pp. 1-12, 1967.

[2] W. J. Book, "Recursive Lagrangian Dynamics of Flexible Manipulator Arms", *International Journal of Robotics Research*, Vol. 3, No. 3, pp. 87-101, 1984.

[3] R. Buckingham, and A. Graham, "Snaking Around in a Nuclear Jungle," *Industrial Robot: An International Journal,* vol. 32, no. 2, pp. 120-127, 2005.

[4] G. Chen, P. M. Tu, T. R. Herve, and C. Prelle, "Design and Modeling of a Micro-Robotic Manipulator for Colonoscopy," *5th Intl. Workshop on Research and Education in Mechatronics*, pp. 109-114, Annecy, France, 2005.

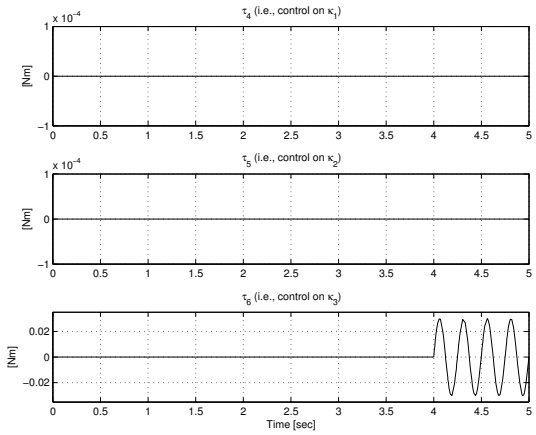

Fig. 5. The control inputs for curvatures (i.e. $\tau_4(t)$, $\tau_5(t)$, $\tau_6(t)$

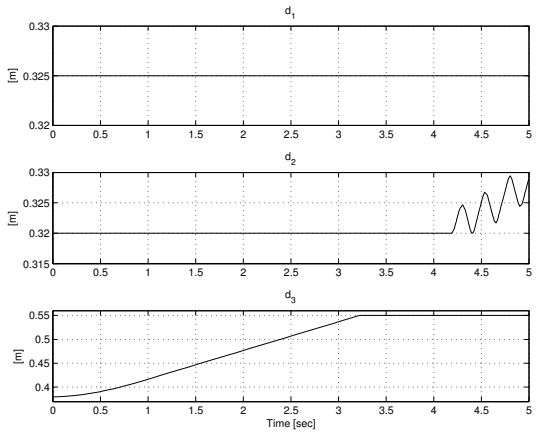

Fig. 6. The section lengths for the second simulation

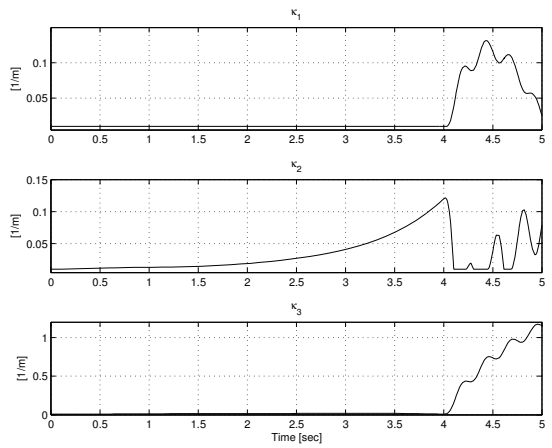

Fig. 7. The curvatures for the second simulation

[5] G. S. Chirikjian, "Hyper-Redundant Manipulator Dynamics: A Continuum Approximation," *Advanced Robotics*, vol. 9, no. 3, pp. 217-243, 1995.

[6] G. S. Chirikjian and J. W. Burdick, "A Hyper-Redundant Manipulator," *IEEE Robotics and Automation Magazine*, Vol. 1, No. 4, pp. 22-29, 1994.

[7] G. S. Chirikjian and J. W. Burdick, "A Modal Approach to Hyper-Redundant Manipulator Kinematics," *IEEE Trans. on Robotics and Automation*, vol. 10, no. 3, pp. 343-354, 1994.

[8] R. Cieslak and A. Morecki, "Elephant Trunk Type Elastic Manipulator a Tool for Bulk and Liquid Type Materials Transportation", *Robotica*, vol. 17, no. 1, pp. 11-16, 1999.

[9] S. Hirose, *Biologically Inspired Robots*, New York, NY: Oxford University Press, 1993.

[10] G. Immega and K. Antonelli, "The KSI Tentacle Manipulator," *Proc. IEEE Intl. Conf. Robotics and Automation*, pp. 3149-3154, Nagoya, Japan, 1995.

[11] M. Ivanescu, N. Popescu, and D. Popescu, "A Variable Length Tentacle Manipulator Control System," *Proc. IEEE Intl. Conf. Robotics and Automation*, pp. 3274-3279, Barcelona, Spain, 2005.

[12] M. Ivanescu and V. Stoian, "A Variable Structure Controller for a Tentacle Manipulator," *Proc. IEEE Intl. Conf. Robotics and Automation*, pp. 3155-3160, Nagoya, Japan, 1995.

[13] B. A. Jones and I. D. Walker, "Kinematics for Multi-Section Continuum Robots," *IEEE Trans. on Robotics*, Vol. 22, No. 1, pp. 43-55, 2006.

[14] B. A. Jones and I. D. Walker, "Limiting-case analysis of continuum trunk kinematics," *Proc. IEEE Intl. Conf. Robotics and Automation*, April 2007, Rome, Italy, to appear.

[15] W. Khalil, G. Gallot, O. Ibrahim, and F. Boyer, "Dynamic Modeling of a 3-D Serial Eel-Like Robot," *Proc. IEEE Intl. Conf. Robotics and Automation*, pp. 1282-1287, Barcelona, Spain, 2005.

[16] D. M. Lane, J. B. C. Davies, G. Robinson, D. J. O'Brien, J. Sneddon, E. Seaton, and A. Elfstrom, "The AMADEUS Dextrous Subsea Hand: Design, Modeling, and Sensor Processing," *IEEE Journal of Oceanic Engineering*, vol. 24, no. 1, pp. 96-111, 1999.

[17] F. Matsuno and H. Sato, "Trajectory Tracking Control of Snake Robots Based on Dynamic Model," *Proc. IEEE Intl. Conf. Robotics and Automation*, pp. 3040-3045, Barcelona, Spain, 2005.

[18] W. McMahan, B. A. Jones, V. Chitrakaran, M. Csencsits, M. Grissom, M. Pritts, C. D. Rahn, and I. D. Walker, "Field Trials and Testing of the OctArm Continuum Manipulator," *Proc. IEEE Intl. Conf. Robotics and Automation*, pp. 2336-2341, Orlando, FL, 2006.

[19] W. McMahan, B. Jones, and I. D. Walker, "Robotic Manipulators Inspired by Cephalopod Limbs," *The Journal of Engineering Design and Innovation*, vol. 1P, paper 01P2, 2005.

[20] H. Mochiyama, T. Suzuki, "Dynamics Modelling of a Hyper-Flexible Manipulator," *Proc. of the 41st SICE Annual Conference*, pp. 1505-1510, Osaka, Japan, 2002.

[21] H. Mochiyama and T. Suzuki, "Kinematics and Dynamics of a Cable-Like Hyper-Flexible Manipulator," *Proc. IEEE Intl. Conf. Robotics and Automation*, pp. 3672-3677, Taipei, Taiwan, 2003.

[22] H. Ohno and S. Hirose, "Design of Slim Slime Robot and Its Gait of Locomotion," *Proc. IEEE/RSJ Intl. Conf. on Intelligent Robots and Systems*, pp. 707-715, Maui, HI, 2001.

[23] G. Robinson and J. B. C. Davies, "Continuum Robots - A State of the Art," *Proc. IEEE Intl. Conf. Robotics and Automation*, pp. 2849-2854, Detroit, MI, 1999.

[24] M. W. Spong, and M. Vidyasagar, *Robot Dynamics and Control*, New York, NY: John Wiley & Sons, Inc., 1989.

[25] K. Suzumori, S. Iikura, and H. Tanaka, "Development of Flexible Microactuator and Its Applications to Robotic Mechanisms," *Proc. IEEE Intl. Conf. Robotics and Automation*, pp. 1622-1627, Sacramento, CA, 1991.

[26] E. Tatlicioglu, I. D. Walker, and D. M. Dawson, "Dynamic Modelling for Planar Extensible Continuum Robot Manipulators," Clemson University CRB Technical Report, CU/CRB/9/15/06/#1, http://www.ces.clemson.edu/ece/crb/publictn/tr.htm, September, 2006.

[27] H. Tsukagoshi, A. Kitagawa, and M. Segawa, "Active Hose: An Artificial Elephant's Nose with Maneuverability for Rescue Operation," *Proc. IEEE Intl. Conf. Robotics and Automation*, pp. 2454-2459, Seoul, Korea, 2001.

[28] I. D. Walker, C. Carreras, R. McDonnell, and G. Grimes, "Extension Versus Bending for Continuum Robots," *Intl. Journal of Advanced Robotic Systems*, vol. 3, no. 2, pp. 171-178, 2006.

[29] Y. Yekutieli, R. Sagiv-Zohar, R. Aharonov, Y. Engel, B. Hochner, and T. Flash, "Dynamic Model of the Octopus Arm. I. Biomechanics of the Octopus Arm Reaching Movement", *Journal of Neurophysiology*, vol. 94, pp. 1443-1458, 2005.